Reactive helicity and reactive power in nanoscale optics

Manuel Nieto-Vesperinas
Instituto de Ciencia de Materiales de Madrid, C.S.I.C.
Cantoblanco, Madrid 28049. Spain.
www.icmm.csic.es/mnv
mnieto@icmm.csic.es

Nanolight Conference
Benasque, March 2022

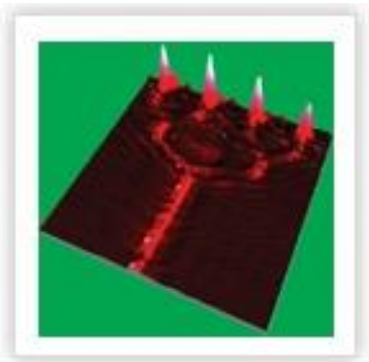

To the memory of Prof. Juan José Sáenz

Thanks to my young collaborator:

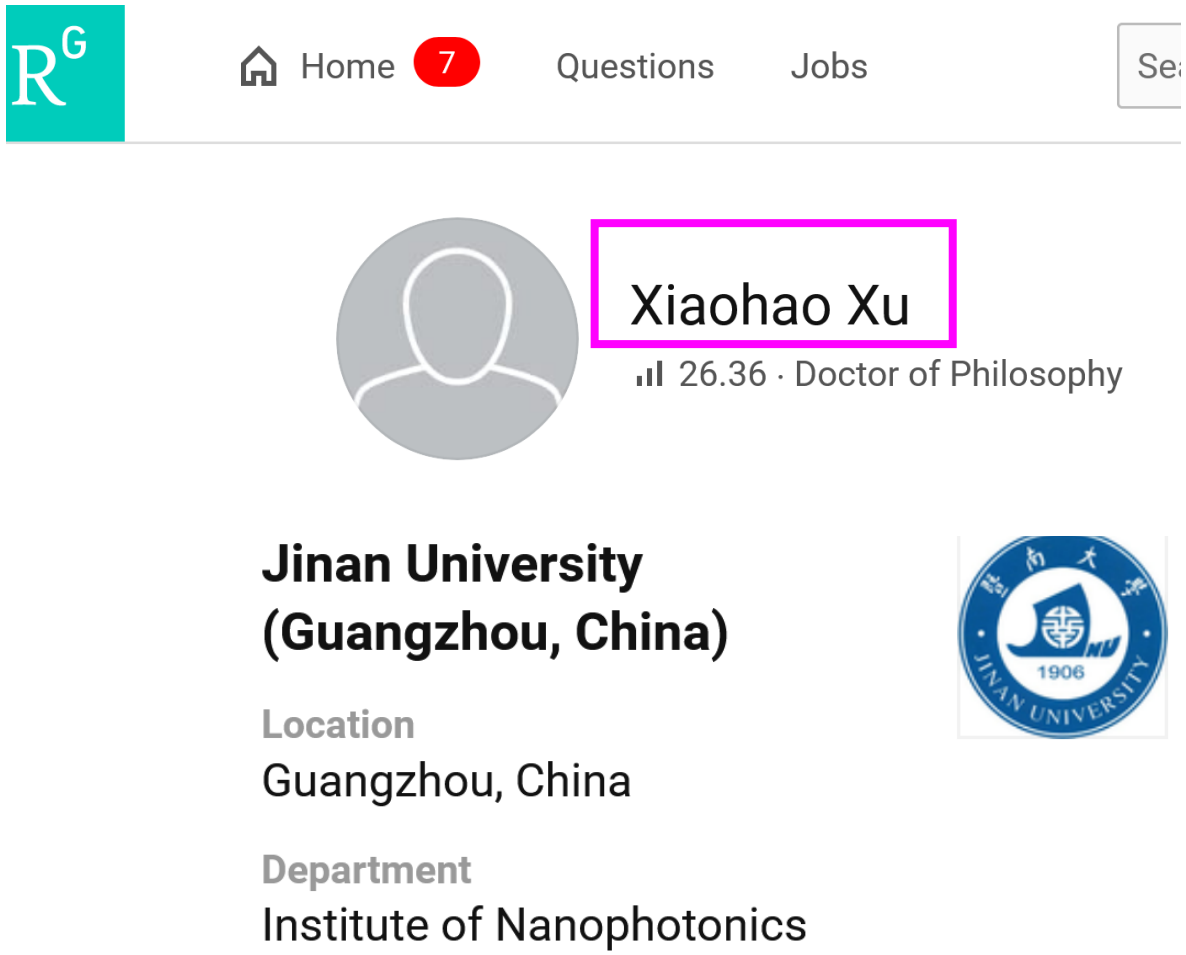

Record:

THE REACTIVE POWER IS A CLASSIC CONCEPT IN ANTENNA THEORY

W. Geyi and P. Jarmuszewski, The foster reactance theorem for antennas and radiation Q, IEEE Trans. Antenn. Propag. **48**, 401 (2000); W. Geyi, *Foundatios of Applied Electrodynamics* (J. Wiley, New York, 2010). Sec. 4.4.1.

WHAT ABOUT AS REGARDS TO THE HELICITY?:

Bliokh, Kivshar, Nori, PRL 113, 033601 (2014) introduce the term: "*Magnetoelectric energy*".
No physical meaning nor physical law provided. No mention of any reactive property.

Kamenetskii, Berezin, Shavit, Appl. Phys. B, 2015, introduce the term: "*Real helicity*".

No physical meaning nor physical law provided. No mention of any reactive property.

WHAT ABOUT NANOANTENNAS?:

A study of reactive quantities: reactive power and reactive helicity aims to controlling dynamic effects (optical forces) in the near-field, and resonances of re-emitted (scattered) energy and helicity.

PHYSICAL REVIEW RESEARCH **3**, 043080 (2021)

Reactive helicity and reactive power in nanoscale optics: Evanescent waves. Kerker conditions. Optical theorems and reactive dichroism

Manuel Nieto-Vesperinas [1,*] and Xiaohao Xu [2,†]

[1] *Instituto de Ciencia de Materiales de Madrid, Consejo Superior de Investigaciones Científicas, Campus de Cantoblanco, Madrid 28049, Spain*

[2] *Institute of Nanophotonics, Jinan University, Guangzhou 511443, China*

(Received 17 June 2021; accepted 6 October 2021; published 28 October 2021)

The Physics of the Reactive Power

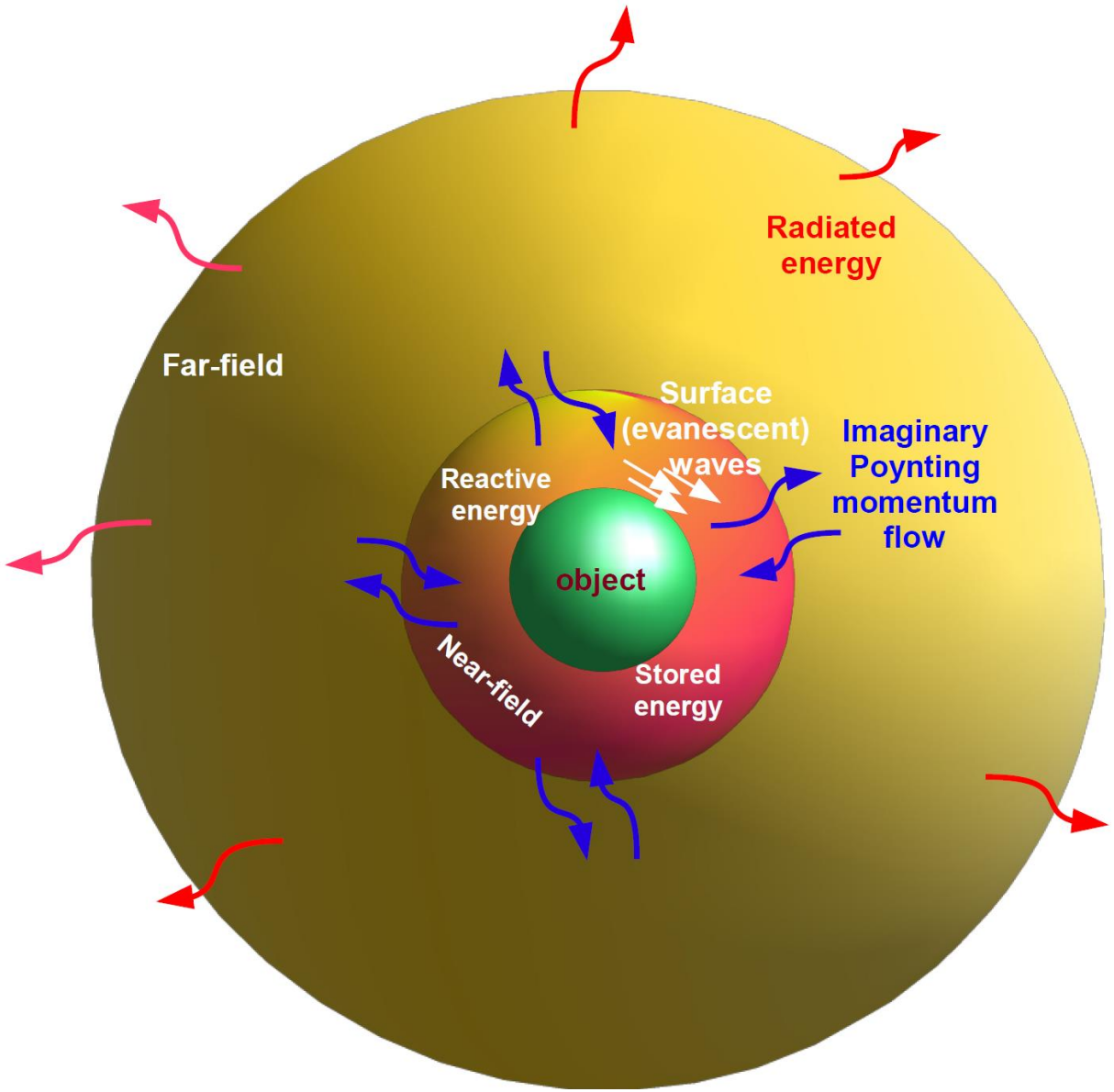

Time-harmonic fields

The fundamentals of antenna theory:

The complex Poynting theorem:

$$\int_V \left[\frac{1}{2}\mathbf{j}^* \cdot \mathbf{E} + \nabla \cdot \mathbf{S}\right] d^3r = i2\omega \int_V (\langle w_m \rangle - \langle w_e \rangle) d^3r$$

Im{**S**} is the reactive (imaginary) Poynting vector. It alternates back and forth from the scattering object at 2ω building-up reactive power: 2ω (<wm>-<we>)

$$\mathbf{S}(\mathbf{r}) = \frac{c}{8\pi\mu}\mathbf{E}(\mathbf{r}) \times \mathbf{B}^*(\mathbf{r}),$$

$$\langle w_e(\mathbf{r}) \rangle = \frac{\epsilon}{16\pi}|\mathbf{E}(\mathbf{r})|^2, \quad \langle w_m(\mathbf{r}) \rangle = \frac{1}{16\pi\mu}|\mathbf{B}(\mathbf{r})|^2.$$

The Physics of the Reactive Helicity

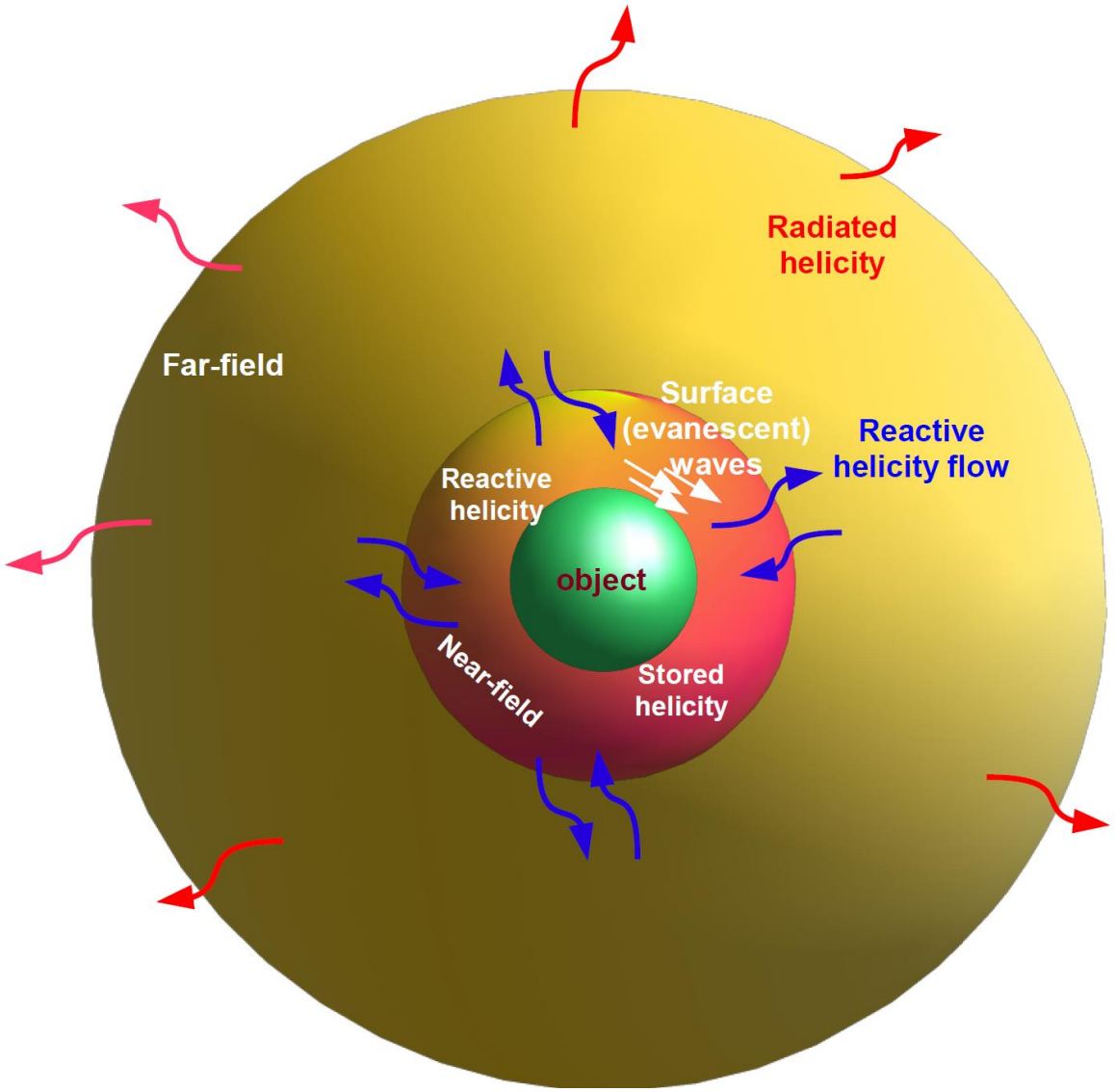

Time-harmonic fields

What about helicity theory?:

MN-V & X. Xu, , PRR **3**, 043080 (2021)

We establish the Reactive Helicity theorem:

$$\int_V \left[-\frac{2\pi}{kn}\mathrm{Im}\{\mathbf{j}^*\cdot\mathbf{B}\} + \nabla\cdot\boldsymbol{\mathcal{F}}_{\mathscr{H}_\mathscr{R}} \right] d^3r = 2\omega \int_V \mathscr{H}_\mathscr{R} d^3r$$

$$\boldsymbol{\mathcal{F}}_{\mathscr{H}_\mathscr{R}} = \boldsymbol{\mathcal{F}}_B - \boldsymbol{\mathcal{F}}_E = (c/4kn)\Im\{\mathbf{H}^*\times\mathbf{B} - \mathbf{E}^*\times\mathbf{D}\}$$

$$= \frac{2\pi c^2}{n}(\langle \boldsymbol{\mathcal{S}}_m\rangle - \langle \boldsymbol{\mathcal{S}}_e\rangle).$$

(Spin angular momenta)

$\boldsymbol{\mathcal{F}}_{\mathscr{H}_\mathscr{R}}$ alternates back and forth from the scattering object at 2ω building-up the reactive helicity:

$$\mathscr{H}_\mathscr{R}(\mathbf{r}) = (1/2k)\sqrt{\frac{\epsilon}{\mu}}\mathrm{Re}\{\mathbf{E}(\mathbf{r})\cdot\mathbf{B}^*(\mathbf{r})\}$$

EVANESCENT WAVE BY T.I.R.

REACTIVE QUANTITIES

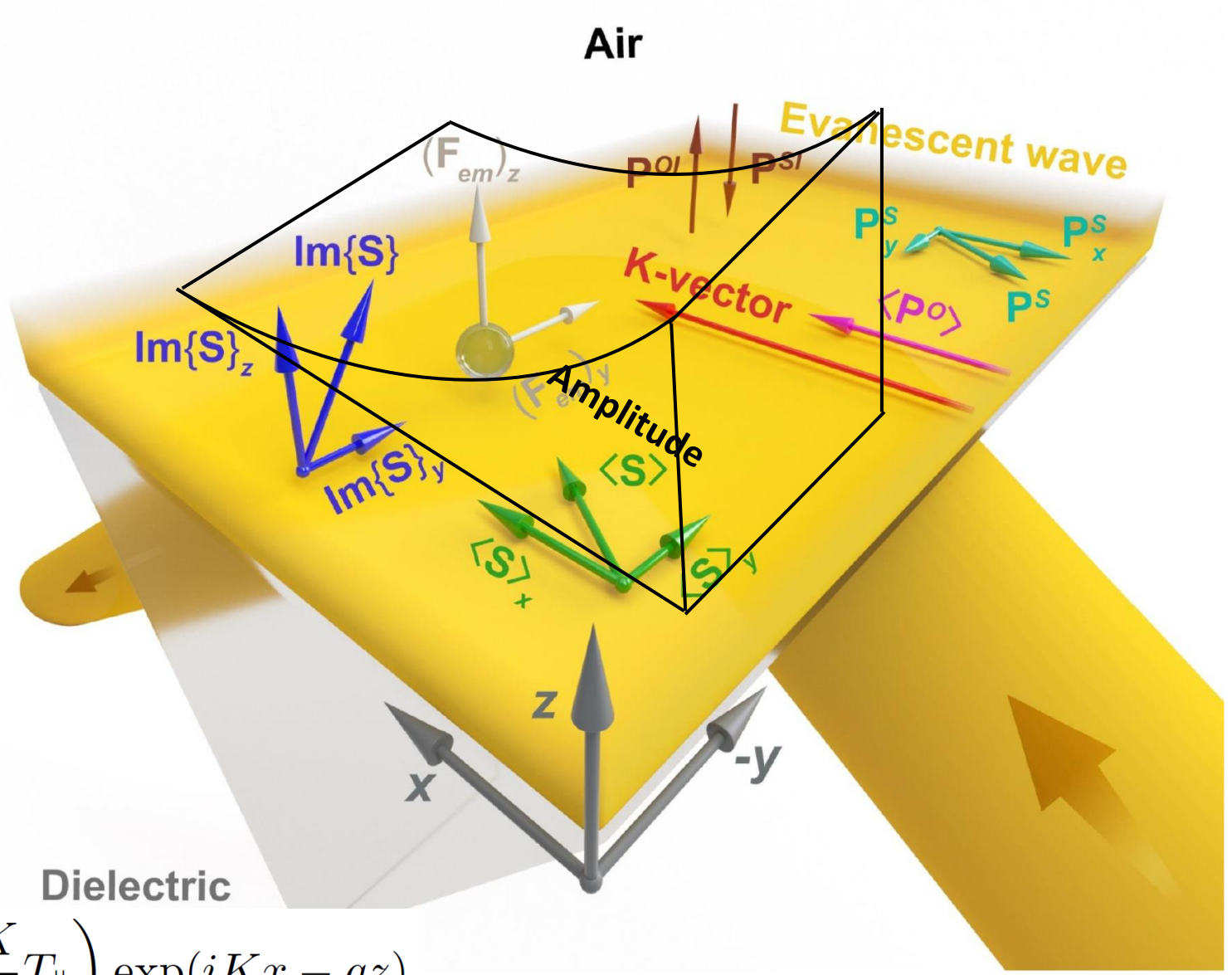

$$\mathbf{E} = \left(-\frac{iq}{k}T_{\parallel}, T_{\perp}, \frac{K}{k}T_{\parallel}\right)\exp(iKx - qz),$$

$$\mathbf{B} = n\left(-\frac{iq}{k}T_{\perp}, -T_{\parallel}, \frac{K}{k}T_{\perp}\right) \times \exp(iKx - qz).$$

$$k(\mathbf{s}_{xy}, s_z) = (K, 0, iq),\ q = \sqrt{K^2 - k^2},\ k^2 = K^2 - q^2.$$

Reactive quantities:

EVANESCENT WAVE BY T.I.R.

$$w_{react} = \frac{c}{4\pi}\frac{q^2}{k}(|T_\perp|^2 - |T_\parallel|^2)\exp(-2qz).$$

$$\mathscr{H}_{\mathscr{R}} = (q^2/k^3)\Re\{T_\perp T_\parallel^*\}\exp(-2qz).$$

Reactive Poynting vector and Reactive Momentum:

$$Im\{\mathbf{S}\} = \frac{1}{2q}[0\,,\frac{ckK}{2\pi}\mathscr{H}_{\mathscr{R}}\,,-w_{react}].$$

$$\mathbf{g}^I = Im\{\mathbf{g}\} = Im\{\mathbf{S}\}/c^2$$

Reactive power conservation:

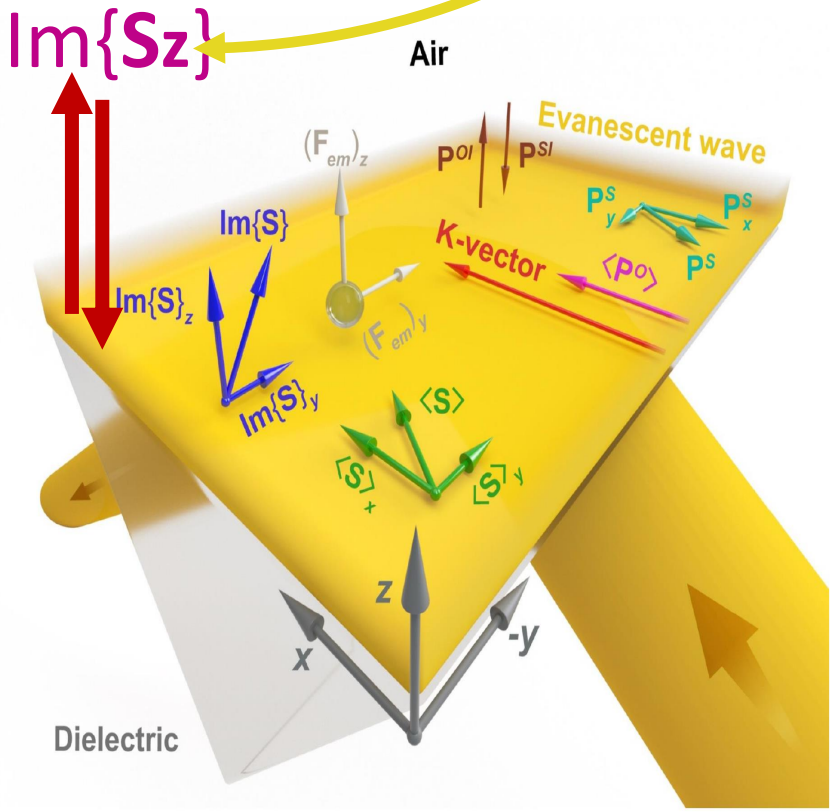

The z-component of $Im\{\mathbf{S}\}$ depends on the *reactive power* density, $\nabla \cdot Im\{\mathbf{S}\}$, of the evanescent wave in the half-space $z > 0$, (which actually concentrates in the *near field* region above the interface $z = 0$, namely at $z << \lambda$), flowing back and forth along OZ at twice the frequency ω, without contributing to a net energy flow since its time-average is zero. I.e. one has from the CPV theorem:

$$\nabla \cdot Im\{\mathbf{S}\} \equiv \partial_z Im\{\mathbf{S}\} = w_{react} \equiv -2qIm\{\mathbf{S}\}_z \, .$$

Reactive helicity conservation:

EVANESCENT WAVE BY T.I.R.

$(\mathcal{F}_{\mathcal{H}_\mathcal{R}})_z$

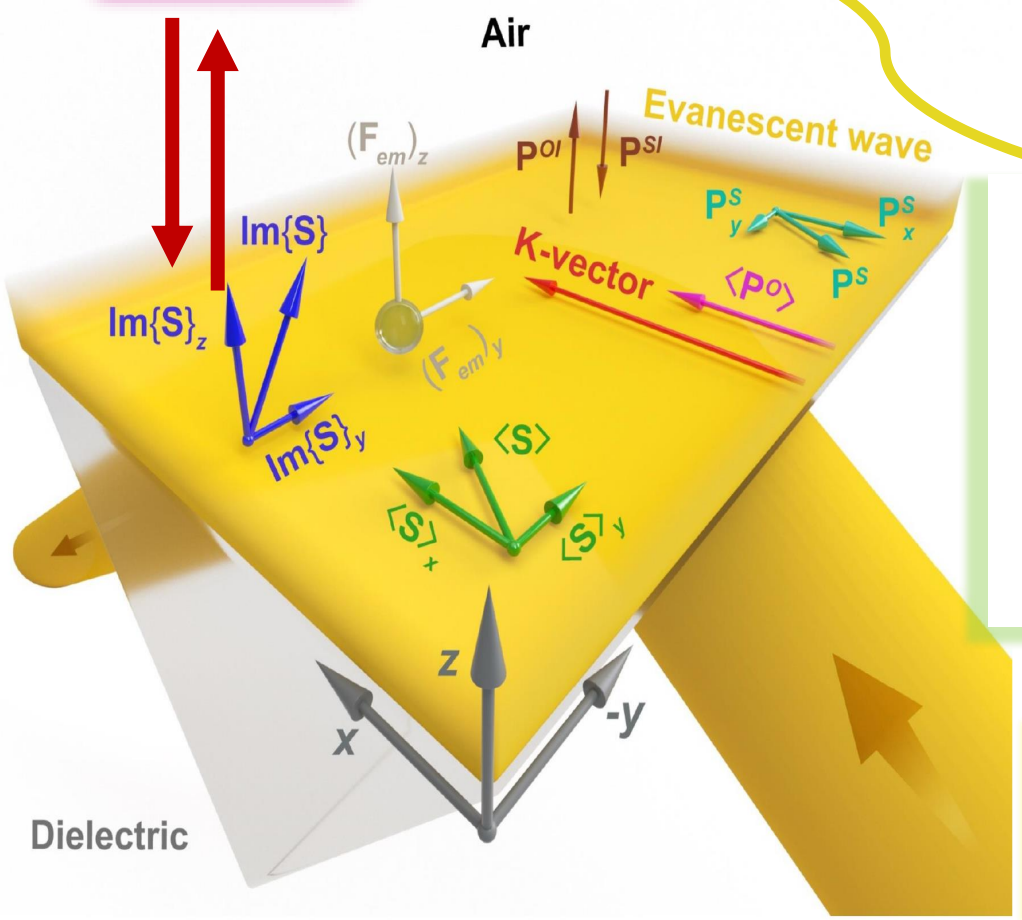

Reactive helicity flow:

$$\mathcal{F}_{\mathcal{H}_\mathcal{R}} = -\frac{1}{q}\left[0\,,\,\frac{2\pi K}{k^2}w_{react}\,,\,ck\mathcal{H}_\mathcal{R}\right].$$

the z-component of $\mathcal{F}_{\mathcal{H}_\mathcal{R}}$ depends on the *reactive helicity* density, $\nabla\cdot\mathcal{F}_{\mathcal{H}_\mathcal{R}}$, of the evanescent wave in the half-space $z>0$, concentrated in the *near field* on $z=0$, flowing up and down in the the z-direction without yielding a net flow since its time-average is zero.

$$\nabla\cdot\mathcal{F}_{\mathcal{H}_\mathcal{R}} \equiv \partial_z\mathcal{F} = -2q(\mathcal{F}_{\mathcal{H}_\mathcal{R}})_z \equiv 2\omega\mathcal{H}_\mathcal{R}\,.$$

REACTIVE QUANTITIES

$\mathbf{g}^I$ whose components come from two vectors that we put forward next: *the density of both reactive spin momentum* $\boldsymbol{\mathcal{P}}^S$ and *reactive orbital momentum* $\boldsymbol{\mathcal{P}}^O$:

$$\boldsymbol{\mathcal{P}}^S = \frac{1}{2}(\mathbf{P}_m^{S\,I} - \mathbf{P}_e^{S\,I}) = \frac{K}{2cq}(0, \frac{k}{2\pi}\mathscr{H}_{\mathscr{R}}, -\frac{K}{ck^2}w_{react}),$$

Superscript ***I*** is imaginary part

$$\boldsymbol{\mathcal{P}}^O = \frac{1}{2}(\mathbf{P}_m^{O\,I} - \mathbf{P}_e^{O\,I}) = \frac{q}{2cq}(0, 0, \frac{q}{ck^2}w_{react}). \qquad (25)$$

P^S and **P^O** are **the spin** and **orbital**, electric or magnetic, momenta Namely,

$$\mathbf{g}^I = \boldsymbol{\mathcal{P}}^S + \boldsymbol{\mathcal{P}}^O. \qquad (26)$$

We emphasize that g_y^I *is fully due to* $\mathcal{P}_y^S$, *while* g_z^I *comes from* $\mathcal{P}_z^S + \mathcal{P}_z^O$.

THE PHYSICS OF THE REACTIVE (IMAGINARY) POYNTING MOMENTUM : OPTICAL FORCES

We shall analyze forces on magnetodielectric particles due to reactive quantities of an evanescent wave. These are its reactive helicity and its flow
and its reactive power and its flow: the Imaginary Poynting momentum.

In our opinión, and as far as we know, these forces have not yet been adequately studied. Whether studied at all.

Such forces, and the upsurge of the reactive quantities, are those due to the interaction between the induced electric and magnetic dipole, that we predicted several years ago, (cf. Op. Ex. 2010), from which the so-called *extraordinary momentum* of evanescent waves was inferred (Bliokh et al. Nat. Comm. 2014), and the force due to it, measured (Antognozzi et al. Nat. Phys. 2016).

Optical force on a magnetodielectric dipolar particle due to the Interaction of the induced electric and magnetic dipole:

MN-V, Juanjo Sáenz, et al., OpEx. 2010

$$< \mathbf{F}_{e-m} >= \frac{8\pi k^4 c}{3}[-Re(\alpha_e \alpha_m^*) < \mathbf{g} > + Im(\alpha_e \alpha_m^*)\mathbf{g}^I].$$

α_e and α_m are the electric and magnetic polarizabilities

Already studied for evanescent waves:
K. Bliokh et al. Nat. Comm. **5,** 3300 (2014). (Prediction).
M. Antognozzi, et al. Nat. Phys. **12**, 731 (2016). (detection).

??

At wavelenghts around the 2nd Kerker condition, the transversal force from $\mathbf{g}^I_y$ is opposite to $<g>_y$!!

Optical force by an on a Si spherical particle placed on the T.I.R. interface due to the reactive field (Poynting) momentum:

EVANESCENT WAVE BY T.I.R.

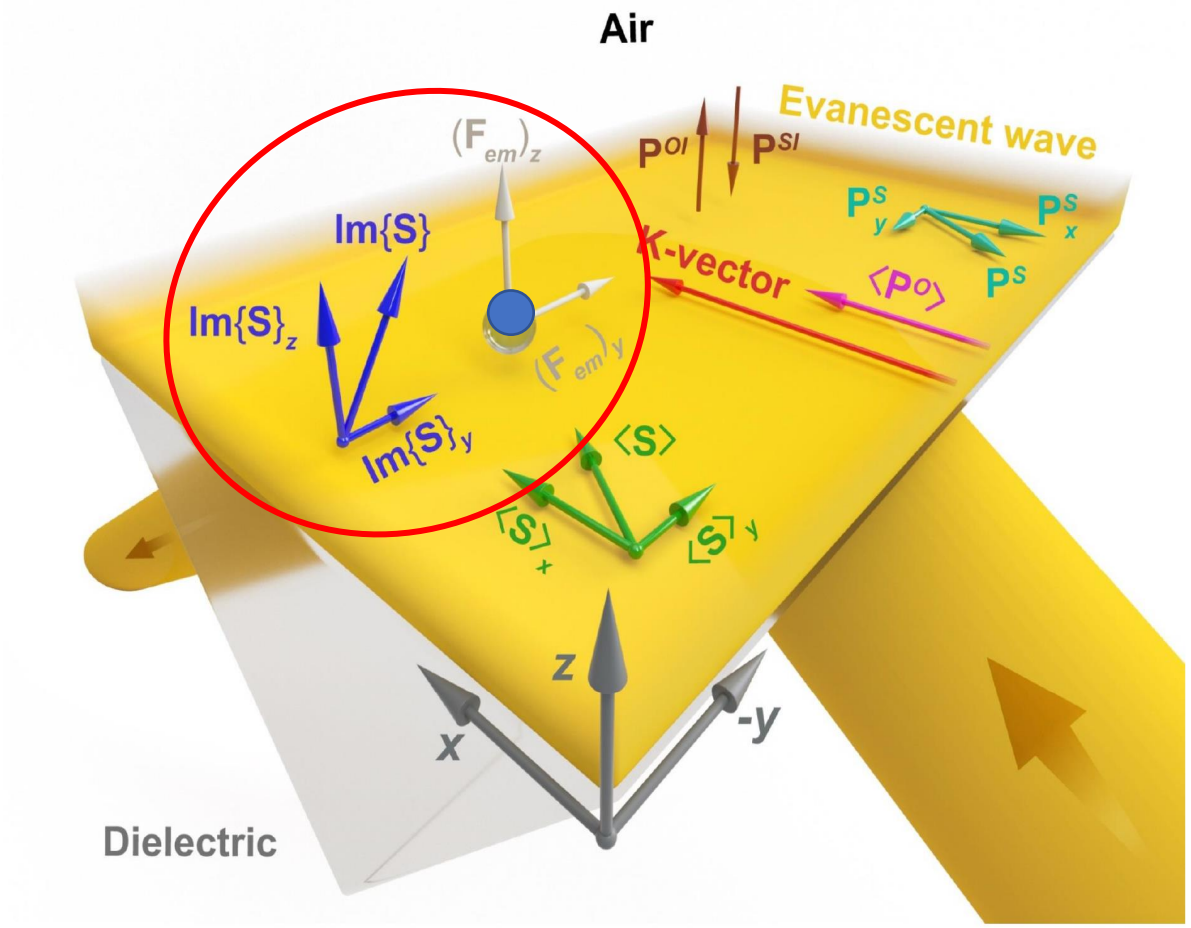

$$< \mathbf{F}_{e-m} >= \frac{8\pi k^4 c}{3} \cdot Im(\alpha_e \alpha_m^*) \mathbf{g}^I$$

$$\mathbf{g}^I = \frac{1}{2qc^2}[0\,, \frac{ckK}{2\pi}\mathscr{H}_{\mathscr{R}}\,, -w_{react}],$$

Transversal component. Considered a secondary weaker force. Not studied in depth.

Perpendicular component

MN-V & X. Xu, , PRR **3**, 043080 (2021)

EVANESCENT WAVE BY T.I.R.

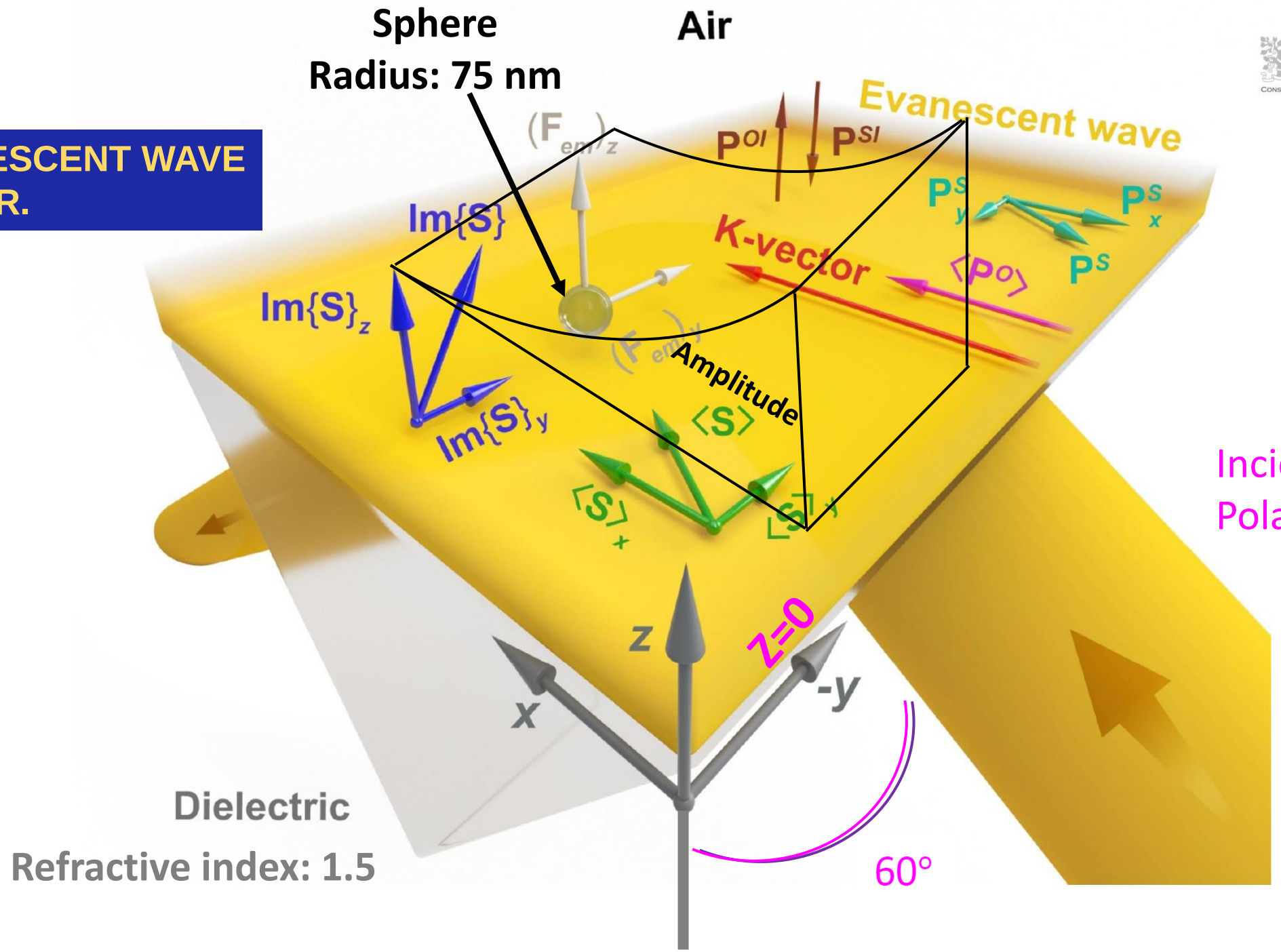

Incident linear Polarization:

$A_{||} = A_{\perp}$

Results for the transversal force due to $\mathbf{g}^I$

MN-V & X. Xu, , PRR **3**, 043080 (2021)

$$< \mathbf{F}_{e-m} >= \frac{8\pi k^4 c}{3} Im(\alpha_e \alpha_m^*) \mathbf{g}^I$$

$$\mathbf{g}^I = \frac{1}{2qc^2}[0\,, \frac{ckK}{2\pi}\mathscr{H}_{\mathscr{R}}\,, -w_{react}],$$

$$< \mathbf{F}_{e-m} >= \frac{8\pi k^4 c}{3} Re(\alpha_e \alpha_m^*) < \mathbf{g} >$$

$$< \mathbf{g} >= \frac{ck}{K}[w\,, -\frac{q}{4\pi}\mathscr{H}\,, 0]/c^2$$

$F_y^{<g>}$

F_y^{gl}

(pN / nm² per incident mW)

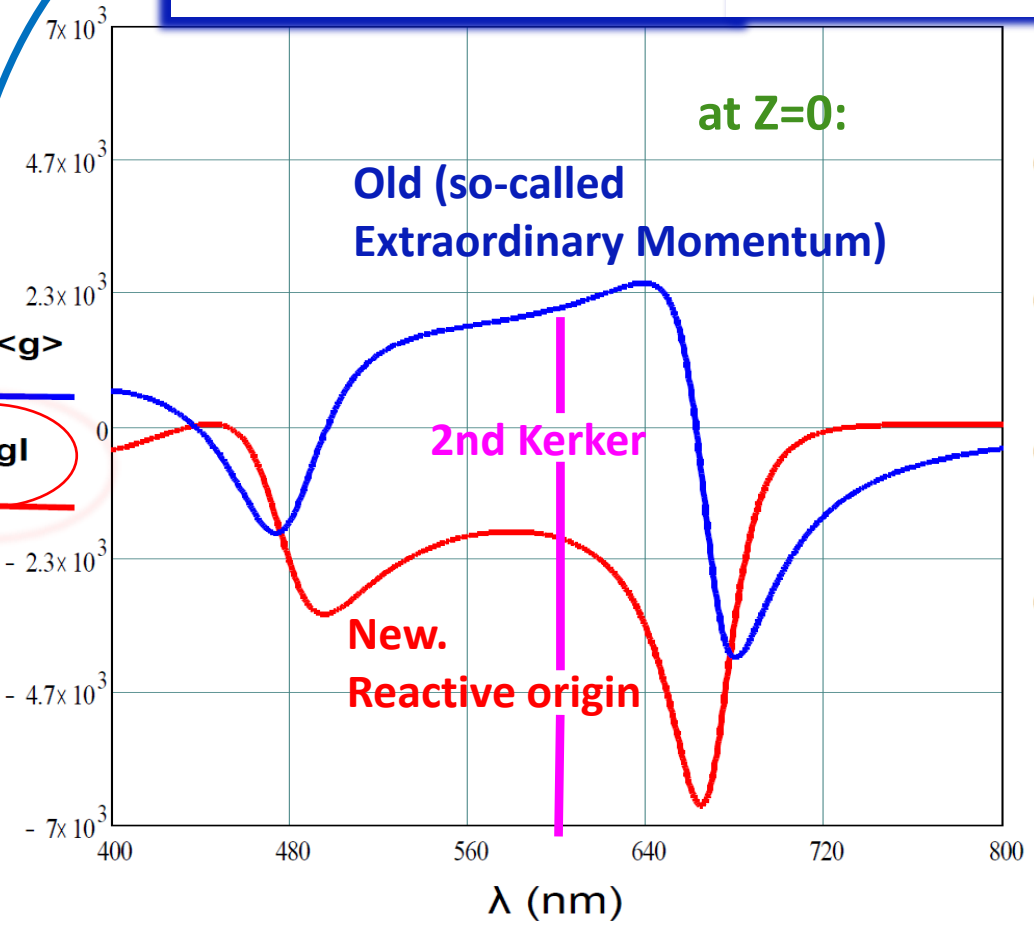

α_e^R/a^3

α_e^I/a^3

α_m^R/a^3

α_m^I/a^3

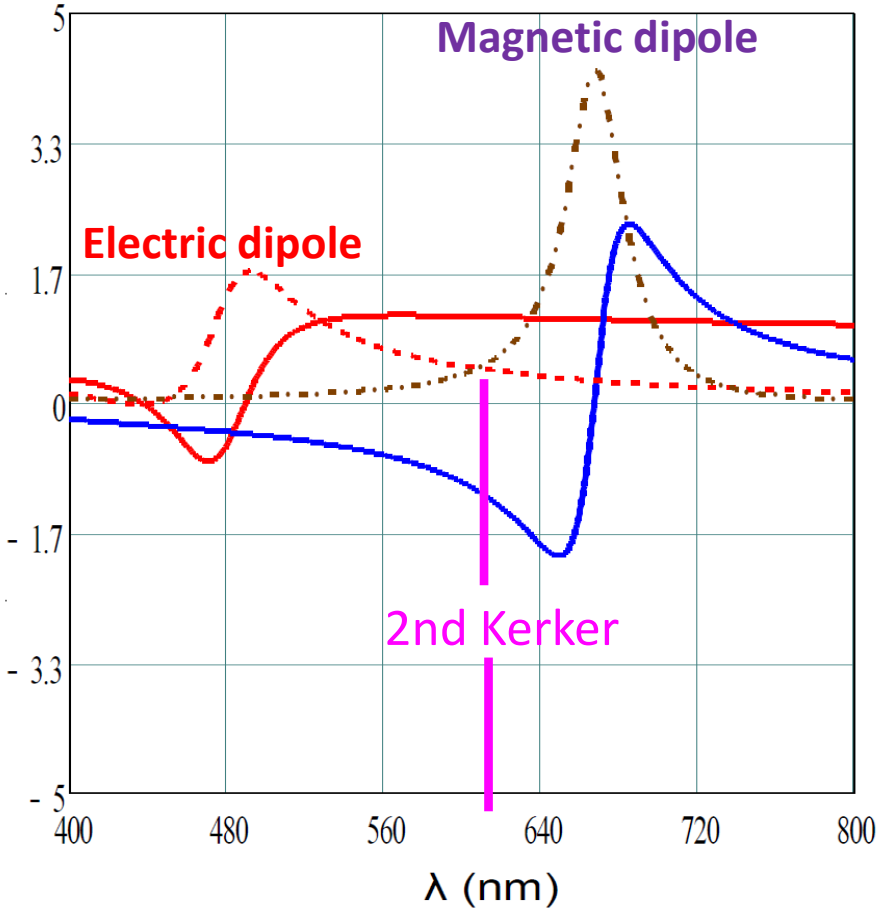

Results for the perpendicular force due to $\mathbf{g}^I$ versus gradient force

$$< \mathbf{F}_{e-m} >= \frac{8\pi k^4 c}{3} Im(\alpha_e \alpha_m^*) \mathbf{g}^I$$

$$\mathbf{g}^I \quad \frac{1}{2qc^2}[0\,,\, \frac{ckK}{2\pi}\mathscr{H}_{\mathscr{R}}\,,\, -w_{react}],$$

Gradient force, normal to interface:

$$< \mathbf{F} >_z^{grad} = -(1/2)\alpha_e^R q |T_\perp|^2 \exp(-2qz)$$

Choose:

$A_{II}=0$

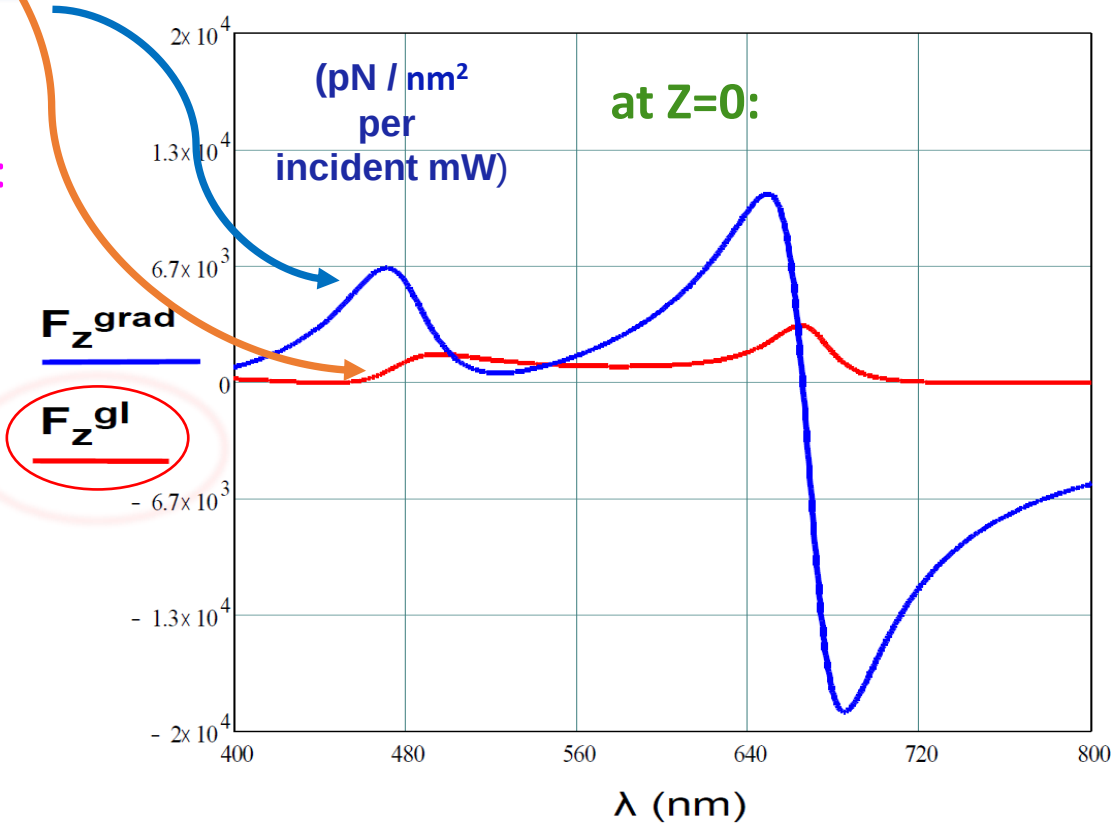

Ratio: $\frac{F_z^{gl}}{F_z^{grad}}$

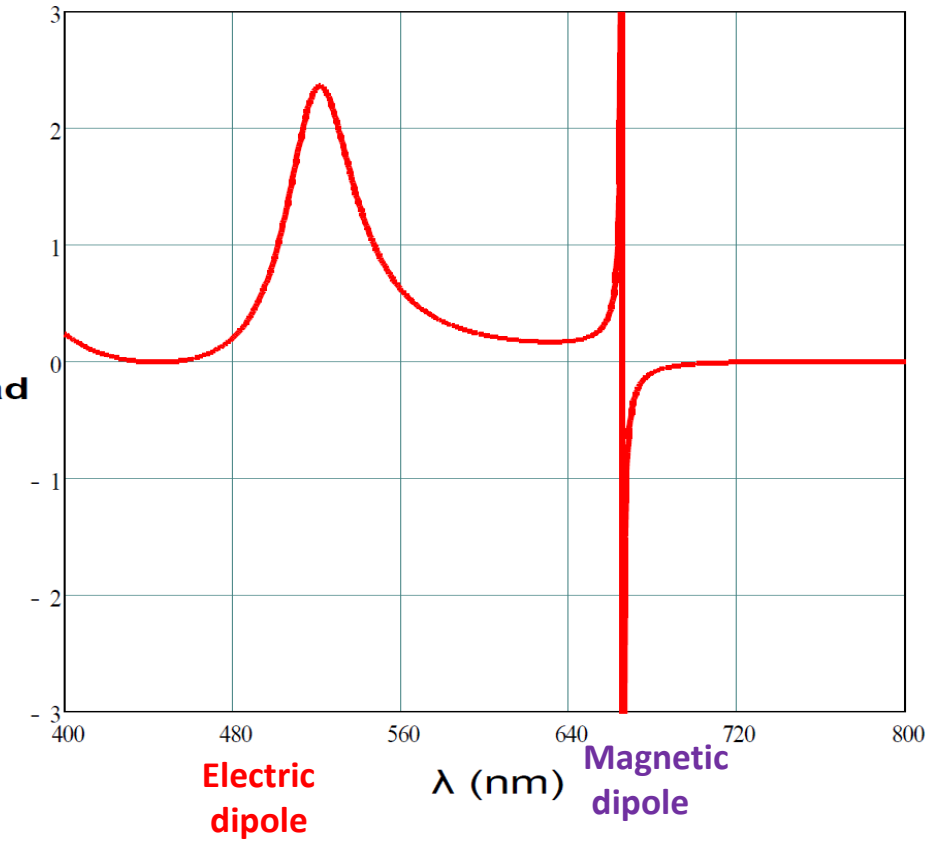

MN-V & X. Xu, , PRR **3**, 043080 (2021)

The field from a dipolar (in the wide sense) particle

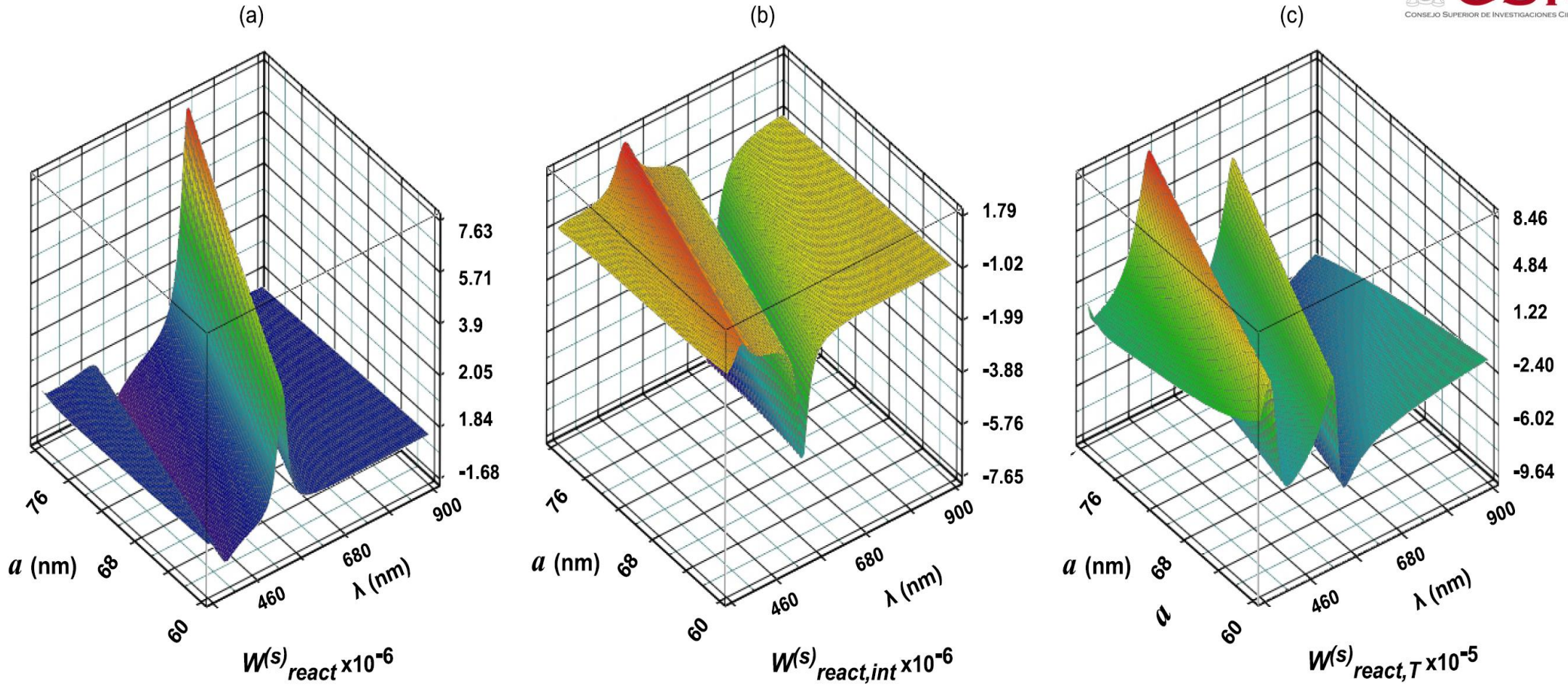

FIG. 3. 3D graphs of reactive powers as functions of wavelength λ and radius a of a magnetodielelectric sphere of Si in air, illuminated by a (linearly or circularly polarized) plane wave. (a): External $W^{(s)}_{\text{react}}$. (b): Interior $W^{(s)}_{\text{react,int}}$. (c): Total $W^{(s)}_{\text{react},T} = W^{(s)}_{\text{react}} + W^{(s)}_{\text{react,int}}$. The sign of $W^{(s)}_{\text{react,int}}$ is opposite to that of $W^{(s)}_{\text{react}}$ for all λ and a. The dip and peak of $W^{(s)}_{\text{react}}$ correspond to the electric and magnetic resonance, respectively, and are close to these resonances in $W^{(s)}_{\text{react,int}}$. Like the resonances exhibited by the scattered power $W^{(s)}$ [46], these peaks and dips are redshifted as a increases. $W^{(s)}_{\text{react},T}$ vanishes in the proximities of these resonances, irrespective of a.

The field from a dipolar (in the wide sense) particle

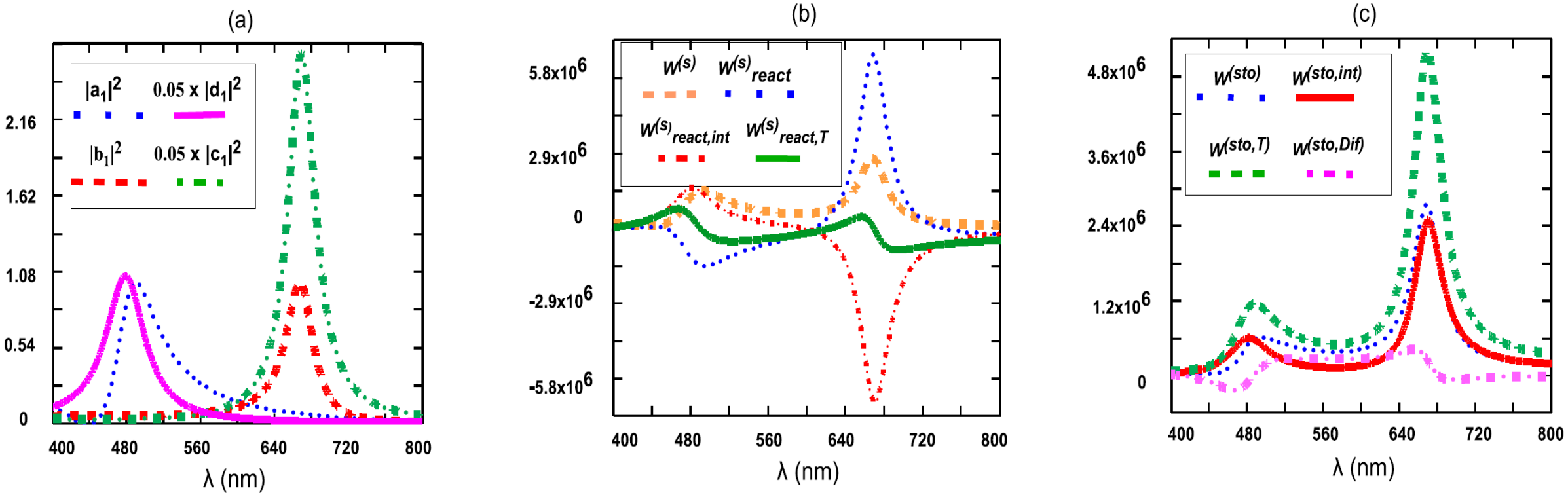

FIG. 4. (a) Si sphere of radius $a = 75$ nm. (a) Square moduli of the electric and magnetic Mie coefficients, a_1 and b_1, and d_1 and c_1 of the external and interior scattered field, respectively. (b) Scattered power $W^{(s)}$ and reactive powers: external $W^{(s)}_{\text{react}}$, interior $W^{(s)}_{\text{react,int}}$, and total $W^{(s)}_{\text{react},T} = W^{(s)}_{\text{react}} + W^{(s)}_{\text{react,int}}$. Notice that $W^{(s)}_{\text{react},T}$ vanishes at wavelenghts close to those of the electric and magnetic Mie resonances: $\lambda_e = 492$ nm and $\lambda_m = 668$ nm, where $W^{(s)}$ is maximum. The lines $|a_1|^2$ and $|b_1|^2$ cross each other at the Kerker wavelengths: $\lambda_{K1} = 738.5$ nm [at which $W^{(s)}_{\text{react}} = 0$ and $W^{(s)}_{\text{react,int}} \simeq 0$] and $\lambda_{K2} = 608$ nm [where both $W^{(s)}_{\text{react}}$ and $W^{(s)}_{\text{react,int}}$ are near 0]. (c) Stored energies: external $W^{(\text{sto})}$, interior $W^{(\text{sto,int})}$, total $W^{(\text{sto},T)} = W^{(\text{sto})} + W^{(\text{sto,int})}$, and difference $W^{(\text{sto,Dif})} = W^{(\text{sto})} - W^{(\text{sto,int})}$.

The field from a dipolar (in the wide sense) particle

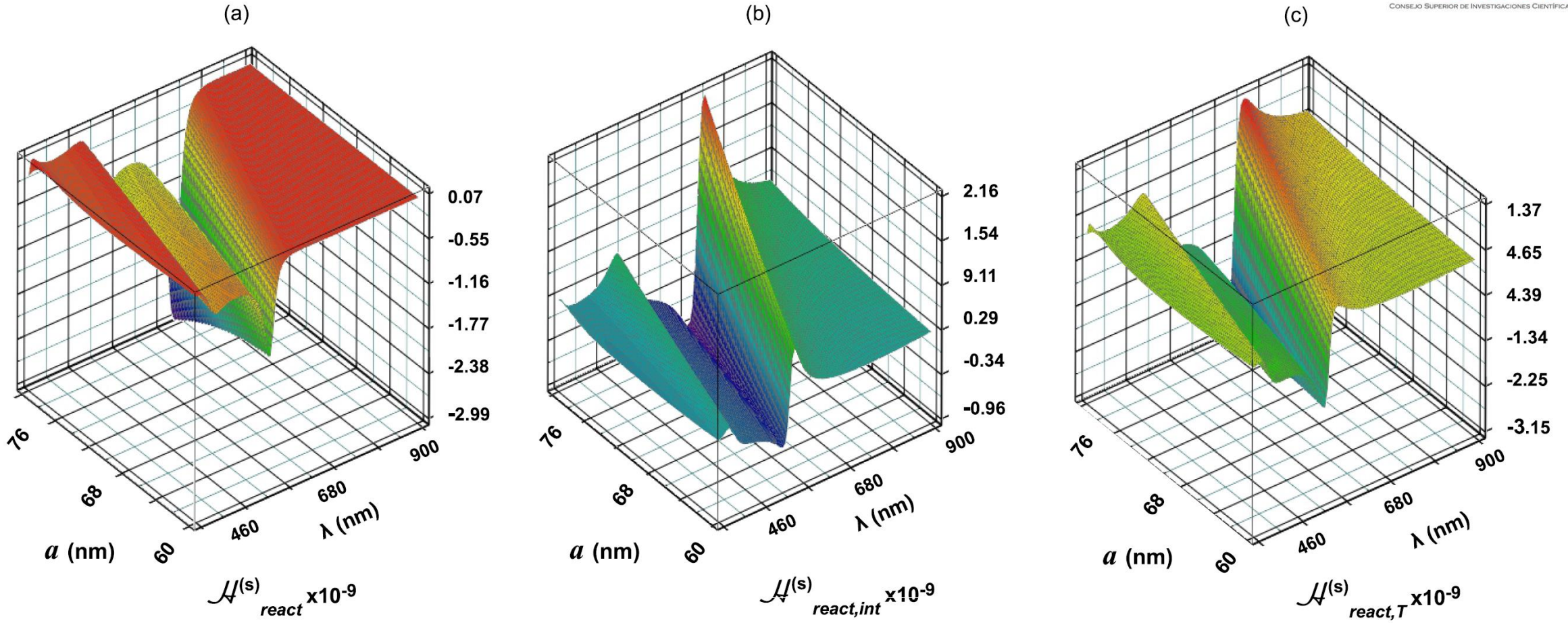

FIG. 5. 3D graphs of reactive helicities as functions of wavelength λ and radius a of a magnetodielelectric sphere of Si in air, illuminated by a left circularly polarized incident plane wave, CPL(+). (a) External $\mathcal{H}^{(s)}_{\text{react}}(\lambda, a)$. (b) Interior $\mathcal{H}^{(s)}_{\text{react,int}}(\lambda, a)$. (c) Total $\mathcal{H}^{(s)}_{\text{react},T}(\lambda, a) = \mathcal{H}^{(s)}_{\text{react}}(\lambda, a) + \mathcal{H}^{(s)}_{\text{react,int}}(\lambda, a)$. The two dips of $\mathcal{H}^{(s)}_{\text{react}}$ and zero crossings of $\mathcal{H}^{(s)}_{\text{react,int}}$ are close to the electric and magnetic resonant wavelengths λ_e and λ_m and are redshifted with increasing a. Irrespective of the value of a, $\mathcal{H}^{(s)}_{\text{react}} = 0$ at λ_{K1} and $\mathcal{H}^{(s)}_{\text{react},T} = 0$ close to λ_e and λ_m.

The field from a dipolar (in the wide sense) particle

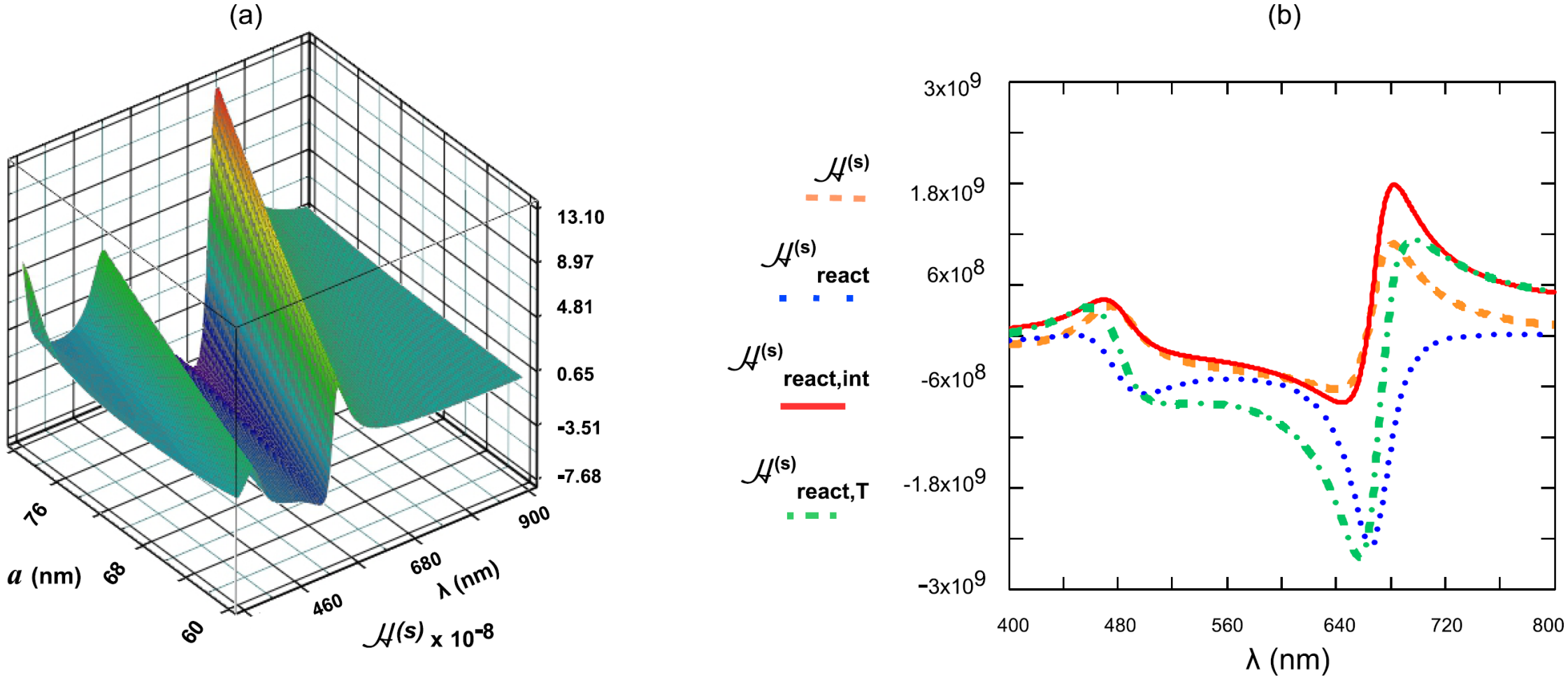

FIG. 6. (a) 3D graph of the scattered helicity $\mathcal{H}^{(s)}(\lambda, a)$ generated by Si spheres in air, illuminated by a left circularly polarized incident plane wave, CPL(+). It has two peaks, at 475 and 679 nm, influenced by the electric and magnetic resonant wavelengths $\lambda_e = 492$ nm and $\lambda_m = 668$ nm. (b) Making $a = 75$ nm, $\mathcal{H}^{(s)}(\lambda)$, $\mathcal{H}^{(s)}_{\text{react}}(\lambda)$, $\mathcal{H}^{(s)}_{\text{react,int}}(\lambda)$, and $\mathcal{H}^{(s)}_{\text{react},T}(\lambda)$. At the Kerker wavelength $\lambda_{K1} = 738.5$ nm, $\mathcal{H}^{(s)}_{\text{react}}$ vanishes. Also $\mathcal{H}^{(s)}_{\text{react},T}(\lambda)$ is zero close to the wavelengths where the scattered helicity $\mathcal{H}^{(s)}$ is maximum, and in the vicinity of extrema of both $\mathcal{H}^{(s)}_{\text{react}}$ and $\mathcal{H}^{(s)}_{\text{react,int}}$.

In conclusión,

¶. Experiments observing these predictions are awaited…

¶. Forces from the electric-magnetic dipole interaction in magnetodielectric particles, and due to reactive quantities of the wavefield, may be larger than those so far observed of the so-called *extraordinary (transversal) momentum* of the evanescent wave; especially in the proximities at the electric and magnetic dipole resonances. They may also neutralize the well-known gradient force.
These forces make observable both the reactive power and reactive helicity.

¶. Reactive quantities yield a novel interpretation of the two Kerker conditions, which are linked to an absence, or minimum, of the overall scattered reactive power.

¶. The reactive helicity of chiral light incident on a chiral nanoparticle may separate enantiomers by excitation of the external reactive power. An effect that we call *reactive dichroism.*